Check for updates

JGR Space Physics

RESEARCH ARTICLE
10.1029/2021JA029936

Key Points:

- Gradient wind balance is dominant in the neutral flow in the auroral oval in disturbed conditions
- The cyclonic flow on the dawn side is severely limited in magnitude by gradient wind constraints
- The anticyclonic flow on the dusk side can show anomalous super-gradient behavior that accommodates significantly larger flow speeds

Correspondence to:
M. F. Larsen,
mlarsen@clemson.edu

Citation:
Larsen, M. F., Pfaff, R. F., Mesquita, R., & Kaeppler, S. R. (2022). Gradient winds and neutral flow dawn-dusk asymmetry in the auroral oval during geomagnetically disturbed conditions. *Journal of Geophysical Research: Space Physics*, *127*, e2021JA029936. https://doi.org/10.1029/2021JA029936

Received 3 SEP 2021
Accepted 6 DEC 2021

© 2021. American Geophysical Union. All Rights Reserved.

Gradient Winds and Neutral Flow Dawn-Dusk Asymmetry in the Auroral Oval During Geomagnetically Disturbed Conditions

M. F. Larsen[1], R. F. Pfaff[2], R. Mesquita[1,3], and S. R. Kaeppler[1]

[1]Department of Physics & Astronomy, Clemson University, Clemson, SC, USA, [2]NASA/Goddard Space Flight Center, Greenbelt, MD, USA, [3]Now at the Johns Hopkins University Applied Physics Laboratory, Laurel, MD, USA

Abstract The Pedersen component of the Lorentz force produces an acceleration that is generally in the zonal direction in much of the dawn and dusk sectors in the auroral oval. During geomagnetically disturbed conditions, as the neutral flow begins to accelerate through the ion drag force and the flow speeds increase, a balance develops in the meridional direction between the Coriolis, curvature, and pressure gradient forces, which are dominant in the lower thermosphere. The gradient wind equation that describes this balance predicts that the cyclonic flow on the dawn side is limited to the so-called regular solution, which has a maximum value of twice the geostrophic wind speed. The anticyclonic flow on the dusk side, on the other hand, can satisfy either the regular or anomalous solution with a transition at twice the geostrophic wind speed. The anomalous flow solutions have wind speeds significantly greater than the transition value, but are limited by the inertial wind value, that is, the value that corresponds to a balance between the curvature and Coriolis forces. The analysis is carried out to show this result, which indicates that a significant quantitative asymmetry is expected between the dawn- and dusk-side flow, as is observed and has been shown in both observations and a number of numerical modeling studies. Implications for the wind distribution of perturbed pressure gradients and inertial instability are discussed.

Plain Language Summary The ion drag "push" in the lower ionosphere in the auroral oval accelerates the winds in the direction that is generally westward on the dusk side of the auroral oval and generally eastward on the dawn side. Forces perpendicular to the ion push include the Coriolis force, the curvature (centrifugal) force, and the pressure gradient, which set up a balance in the north-south direction that ideally keeps the flow in the acceleration channel. On the evening side the balance of forces is very effective in doing that, but it is shown that on the morning side the balance is limited to a range of wind speeds between zero and twice the geostrophic value. The balance of forces on the evening side can accommodate much larger wind speeds, but even there, the maximum flow speed is limited by the inertial value, which is the wind speed that corresponds to a balance between the centrifugal and Coriolis forces with a value for typical parameters of approximately 350 ms^{-1}. The maximum flow speeds on both the dusk and dawn side are ultimately limited by inertial instability in the flow, which develops if the limits are exceeded.

1. Introduction

Observations dating back at least to the 1970's (e.g., Mikkelsen, Jørgensen, Kelley, Larsen, & Pereira, 1981) have shown that very large winds exceeding 300 ms^{-1} can develop on the dusk side of the auroral oval in the lower *E*-region in active conditions. Joule heating may contribute in part to the acceleration of the winds, but the Pedersen component of the Lorentz force is clearly the dominant force, with ion drifts driven by magnetospheric forcing leading to winds that are closely aligned to the direction of the plasma drifts. The neutral momentum equations, including the Lorentz force terms, were derived by Larsen and Walterscheid (1995), for example, The Pedersen component of the force is that part that depends directly on the Pedersen conductivity. The winds that develop on the dusk side have much in common with the jets that occur near the tropopause in the lower atmosphere in that they have large wind speeds over a limited horizontal extent along the direction of the flow and divergence and convergence associated with the entrance and exit regions of the jets, respectively. Furthermore, the observed wind maxima generally have a peak near 120 to 125 km altitude, which supports the characterization of the feature as being jet-like.

The primary driver for these auroral jets is clearly the Pedersen component of the Lorentz force, but a simple "push" from the ions is not sufficient to be effective in accelerating the winds. In addition to the driving force, a balance of forces is required in the cross-flow direction to keep the air in the acceleration channel and to maintain a stable configuration during the extended time period required for the forcing to have a significant effect. At low speeds, the Coriolis force, which is linearly proportional to the wind speed, is dominant. In particular, an approximate balance generally develops between the Coriolis force and the pressure gradient force. The ambient pressure gradient can contribute to or inhibit the balance, but in either case, the initial deflection of the air parcels in the cross-flow direction increases as the wind speeds increase and lead to back-pressure gradients at the edges of the acceleration channel until a balance is achieved. The adjustment process was described in detail in the early papers by Larsen and Mikkelsen (1983) and Walterscheid and Boucher (1984). The more recent paper by Kwak and Richmond (2007) also gives a clear summary of the dynamics responsible for the adjustment that leads to a balance of forces.

As the wind speeds increase further due to the imposed Lorentz force, the centrifugal force becomes increasingly important for a flow that is zonal or very nearly zonal, as is the case on the dusk side of the auroral oval. In that part of the oval, the balance of forces is particularly favorable since the flow is westward, producing a Coriolis force that is poleward and a centrifugal force that is equatorward. In that case, the re-distribution of mass required for the pressure gradient to complete the balance is relatively minor, and the neutral flow is more likely to stay in the acceleration channel where the Lorentz force can have a great effect.

The situation on the dawn side is much less favorable for the balance of forces required for the imposed Lorentz forcing to be effective. The plasma drifts on that side are generally eastward, which should lead to the development of eastward or nearly eastward neutral flow, but that flow direction leads to both a Coriolis deflection and a centrifugal force that are equatorward. A much greater re-arrangement of mass is therefore required to complete the balance of forces, and the flow tends to be displaced out of the acceleration channel before the Lorentz force has sufficient time to have a significant effect. The general asymmetry between the neutral flow on the dusk and dawn sides of the auroral oval has been noted in various earlier papers dealing with both observational data and modeling studies. An early, excellent example of the asymmetry can be found in the modeling study by Fuller-Rowell and Rees (1981). Gundlach et al. (1988) used a simple shallow-water numerical model to illustrate the effects of the nonlinear centrifugal terms in accounting for the differences in the adjustment process on the dusk and dawn side. The model results presented by Kwak and Richmond (2007) also clearly show the asymmetry, and that paper discusses the associated dynamics.

A major motivation for the results presented here is the Auroral Jets rocket experiment that was carried out in Alaska on 2 March 2017 in the evening sector during a period of enhanced geomagnetic activity. The specific objectives of the experiment were to obtain measurements of the large winds associated with a lower thermosphere jet, as well as in-situ and ground-based measurements of the forcing that contributes to the development of the jet structures. The primary wind measurements were obtained with the trimethyl aluminum tracer technique and showed maximum wind speeds exceeding 300 ms^{-1} with a peak near 120 km altitude where the Pedersen component of the Lorentz force is most effective. The analysis presented here focuses on aspects of the wind balance in auroral jets, the dawn/dusk wind asymmetry, and acceleration effects that can be inferred directly from the gradient wind balance conditions, that is, from a flow characterized by a balance between the Coriolis, centrifugal, and pressure gradient forces, but with aspects that have not been considered in detail in earlier studies. In particular, we show that the development of the very large winds that occur on the dusk side almost certainly require that the balance corresponds to what is referred to as the anomalous gradient wind solution for anticyclonic flow. Because there is no corresponding anomalous solution for cyclonic flow, that is, the flow condition on the dawn side, the asymmetry between the two regions is shown to be a natural consequence of the simple mathematical solution of the gradient wind balance equation. A further consequence of the anomalous solution is that, once the maximum wind speed for the normal solution has been reached, a further decrease in the magnitude of the cross-flow pressure gradient will lead to an increase in the magnitude of the wind that can be accommodated in the balanced state for the anomalous solution, which again makes the Lorentz force more effective and is conducive to the development of large wind speeds.

Two representative examples of evening-side auroral jet observations are presented in the next section. The gradient wind equation analysis is presented after that, including the anomalous solutions and the wind value that represents the transition from the regular to the anomalous flow solution. An analysis of the implications

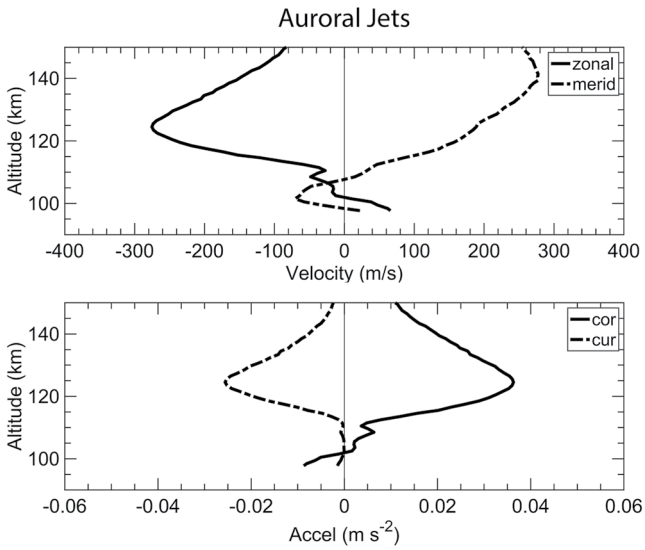

Figure 1. Top panel shows profile of the zonal and meridional winds obtained on the up-leg in the launch on 2 March 2017 from Poker Flat, Alaska. The lower panel shows the calculated Coriolis and curvature accelerations calculated from the measured winds.

for the effect of back-pressures on the flow follows based on a third set of observations, along with a consideration of possible instabilities associated with flow that would limit the maximum flow speed. Finally, the results are summarized and the implications are discussed.

2. Auroral Jets Winds

Jets are ubiquitous in planetary atmospheres, including the Earth's (e.g., Galperin & Read, 2019). Jets that occur in the lower atmosphere near the tropopause are the result of strong horizontal temperature gradients within the larger-scale global temperature gradient. Enhanced wind speeds that characterize the jet stream are the result of synoptic scale instabilities in the flow that create enhanced temperature gradients and strengthen the flow. While similar instabilities may occur in the lower thermosphere, the jets that are the focus of this study are generated primarily by the Pedersen component of the magnetospherically-induced Lorentz force at high latitudes. The increase in plasma density and DC electric fields in active conditions leads to acceleration of the neutrals in the lower *E*-region via neutral-ion collisions in a direction that is close to or in the direction of the plasma flow. To the extent that the neutrals respond directly to the forcing, the neutral acceleration therefore would ideally produce a neutral circulation that mimics the two-cell plasma convection pattern in the auroral oval and polar cap region, although with a temporal lag characterized by the neutral-ion collision frequency. The observations by Heppner and Miller (1982) of high-latitude *F*-region winds showed direct evidence of the time lag shift in the neutral flow pattern response at those heights. The simulation by Crowley et al. (2006), for example, gives examples of the time lag for the *E*-region flow. The time lag depends on geophysical conditions, as can be seen by comparing Figures 2 and 3 of the latter paper. The horizontal north/south scale of the forcing within the dusk or dawn sector in the oval is comparable to the width of the auroral oval. The zonal extent of the acceleration region is limited, at a maximum, by the distance between the sharp turning points in the forcing near the Harang discontinuity and the dayside cusp, although typically the forcing varies longitudinally at shorter scales than that due to variations in the forcing imposed by magnetospheric processes.

To the extent that the neutrals have time to respond to the Lorentz forcing, strong winds will be created in a region with a narrow north/south extent of one hundred to a few hundred kilometers and a much larger longitudinal extent, that is, a flow with the characteristics typical of a jet. In order for the Lorentz force to be effective in accelerating the neutrals significantly it is necessary for the neutrals to remain in the narrow channel where the acceleration occurs for an extended period. Time constants for Pedersen acceleration are an hour or more, even in disturbed conditions (see, e.g., Larsen & Walterscheid, 1995). Any significant net cross-channel flow will tend to move the neutral flow out of the acceleration channel, thus reducing the effectiveness of the forcing in producing enhanced winds.

In this section we present the measurements from two cases that illustrate the jet structure, and the balance of forces that made the acceleration effective. A third case that illustrates the effect of cross-flow advection gradients is shown in a later section. All three sets of measurements were obtained with the sounding rocket vapor tracer technique. The latter provides high-resolution altitude profiles of the winds with relatively small error bars of ~5–10 ms^{-1}. Furthermore, trails released on the up-leg and down-leg portion of the sounding rocket flights typically result in wind profile measurements 100–200 km apart, which is comparable to the width of the forcing region. All three cases shown here are from measurements on the evening side of the auroral oval in Alaska.

The first case is from the Auroral Jets launch that provided the motivation for the overall analysis presented here. The launch was at 0550 UT on 2 March 2017, corresponding to 1840 MLT on March 1, that is, on the dusk side of the auroral oval. The up-leg wind profile in the upper panel of Figure 1 shows strong westward winds that peak near 125 km altitude. The winds gradually rotate toward northward at higher altitudes above that. The down-leg wind profile is not presented here but shows a similar vertical structure and comparable magnitudes in the wind components. The measurements were made during active conditions. Details about the magnetic activity and the

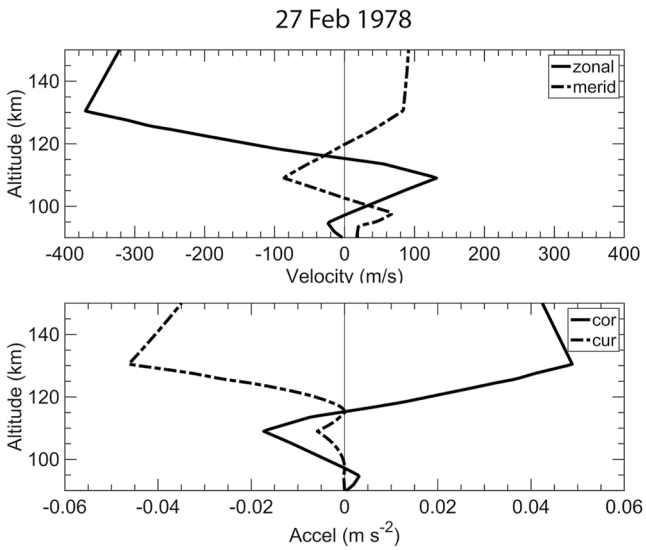

Figure 2. Wind profile and corresponding curvature and Coriolis force profiles from a rocket measurement on 28 Feburary 1978 at Poker Flat, Alaska. Format is the same as in Figure 1.

Lorentz forcing can be found in the dissertation by Mesquita (2021) and will not be presented here. The lower panel in the figure shows the profiles of the meridional components of the Coriolis and curvature terms. The height variation in the two profiles is very similar and the magnitudes are nearly equal and opposite, suggesting a balance in the forces that tends to keep the air in the acceleration channel. The balance of forces for the down-leg profile was very similar in the height variation and force magnitudes. It should be noted that the curvature term calculated here is based on the radial distance from the Earth's rotation axis. The value therefore corresponds to the centrifugal acceleration for a flow along the auroral oval at a constant latitude but is a lower limit since the value can be higher, that is, the effective radius smaller, for an actual circulation with a tighter radius of curvature.

The second case corresponds to a wind profile measured on 28 Feburary 1978, at Poker Flat, Alaska, at 0417 UT in conditions that were more active than in the Auroral Jets case presented above. The time of the launch corresponded to 1717 MLT on Feburary. 27. Details of the forcing and more detailed information about the observations can be found in the papers by Mikkelsen, Jørgensen, Kelley, Larsen, Pereira, Vickrey, et al. (1981); Mikkelsen, Jørgensen, Kelley, Larsen, Pereira, et al. (1981). As described in those papers, winds were measured on two separate nights four days apart close to the same local time. Both launches were in similar activity levels. The profiles in both cases had similar vertical structure and comparable maximum wind speeds. The calculated curvature and Coriolis force profiles are shown in the lower panel of Figure 2. The paper by Mikkelsen, Jørgensen, Kelley, Larsen, Pereira, Vickrey, et al. (1981) included profiles of the various different forces in play, concluding that the Coriolis and curvature terms were in near balance, as shown by the curves presented here.

Various numerical modeling studies have shown that winds in the auroral oval, especially on the dusk side, are in near gradient wind balance. A particularly clear discussion of this point is the paper by Kwak and Richmond (2007), and references therein. The earlier papers, however, have invoked the gradient wind balance qualitatively. More detailed conclusions can be drawn about both the nature of the balance of forces and the response of the atmosphere to the magnetospherically-induced forcing from the analysis of the gradient wind balance equation, as shown in the next section.

3. The Gradient Wind Equation

In response to an imposed Pedersen Lorentz force in the zonal direction the neutrals will begin to accelerate in the direction of the plasma flow within the channel where the electric fields and plasma densities are enhanced, leading to an adjustment process that was discussed by Larsen and Mikkelsen (1983) and Walterscheid and Boucher (1984). Initially, when the wind speeds are still small, the Coriolis force will be dominant, leading to a displacement of the flow in the cross-channel, that is, meridional, direction. Since the flow outside the acceleration channel is stationary or slow moving, convergence occurs on one side of the channel and divergence on the other, producing a back-pressure. A balance between the resulting meridional pressure gradient and the Coriolis force will tend to keep the air parcels in the acceleration channel. The process is transient, however, and as the winds continue to accelerate, the curvature term becomes important so that the meridional balance includes the Coriolis, curvature, and pressure gradient force. A balance between those three forces represents the standard gradient wind balance that is also common in flows in the lower atmosphere, including those associated with curving jet streams and tropical storms. Viscosity becomes increasingly important with altitude in the thermosphere but can be neglected in the lower part of the *E*-region, that is, in the height range of interest here, for the relatively short time scales of a few hours or less required to accelerate the winds to the speeds shown in the two examples above. The Pedersen component of the imposed Lorentz force is therefore a primary driver in the zonal direction, but the key to making that driver effective is the gradient wind balance in the meridional direction that will either keep the air parcels in the acceleration channel if a balance is achieved or push them out of the channel if the forces are not balanced.

Table 1
Roots of the Gradient Wind Equation

	$R > 0$	$R < 0$
$\partial p/\partial n > 0$	Pos root (unphysical)	Pos root (anomalous low)
	Neg root (unphysical)	Neg root (unphysical)
$\partial p/\partial n < 0$	Pos root (normal low)	Pos root (anomalous high)
	Neg root (unphysical)	Neg root (normal high)

The standard solution of the gradient wind equation can be found in a number of texts on atmospheric dynamics or synoptic meteorology, including the one by Holton (1992). We repeat it here since the so-called anomalous solution, which is not commonly considered to be relevant in the lower atmosphere, is of particular interest for the case of the high-latitude thermosphere. The balance of forces can be written as

$$\frac{V^2}{R} + fV + \frac{1}{\rho}\frac{\partial p}{\partial n} = 0 \tag{1}$$

with V the zonal wind speed, R the radius of curvature for the flow, ρ the atmospheric density, p the pressure, and n the normal coordinate, that is, the meridional component in this case, and f is the Coriolis parameter. The equation is quadratic in V. The gradient wind solution is

$$V_{gw} = -\frac{fR}{2} \pm \left(\frac{f^2R^2}{4} - \frac{R}{\rho}\frac{\partial p}{\partial n}\right)^{1/2} \tag{2}$$

Special limiting cases for the flow are a geostrophic balance in which the Coriolis force balances the pressure gradient force so that

$$V_{geo} = -\frac{1}{f\rho}\frac{\partial p}{\partial n} \tag{3}$$

and an inertial balance in which the centrifugal force balances the Coriolis force so that

$$\frac{V^2}{R} + fV = 0 \tag{4}$$

and the inertial wind speed is

$$V_{iner} = -fR \tag{5}$$

The latter is a special case corresponding to either $R \to \infty$ or $\partial p/\partial n \to 0$. The former condition is not especially relevant to the flow solutions in the auroral oval, but the latter is, as we will show below. We can write the solution in terms of the geostrophic and inertial wind, which then takes the form

$$\frac{V_{gw}}{V_{iner}} = -\frac{1}{2}(\mathrm{sgn}R) \pm \left(\frac{1}{4} - \frac{V_{geo}}{V_{iner}}\right)^{1/2} \tag{6}$$

The quadratic equation has only two solutions, corresponding to the +/− signs, but the usual approach is to give R a sign to account for the direction of V_{iner}, that is, east (positive) or west (negative), and a sign for V_{geo}, corresponding to the sign of the pressure gradient, that is, radially inward or outward. Including the two signs for R and the two signs for the pressure gradient, manifested as the sign of V_{geo} in this case, we get eight solutions, but only four are physical. The solutions are given by, for example, Holton (1992), (pp.67–69) and are summarized in Table 1.

The gradient wind directions and balance of forces are shown schematically in Figure 3 for the cases corresponding to the normal gradient wind solutions. The flow and force directions are shown in the context of the two-cell pattern. On the dusk side, the electric fields are poleward, leading to a westward plasma drift and a circulation that is clockwise, corresponding to normal anticyclonic flow in the northern hemisphere. The electric fields are equatorward on the dawn side leading to an eastward plasma drift and a circulation the is counterclockwise in the northern hemisphere, corresponding to normal cyclonic flow. An indication of the pressure gradients expected in each cell can be found in the figures in the article by Crowley et al. (2006), which show several examples of the densities from numerical model simulations. The density maps are consistent with a pattern that has high pressure in the dusk-side cell and low pressure in the dawn-side cell, as shown by the **H** and **L** symbols in Figure 3. The resulting pressure gradient force is represented by the green arrow. The black arrow shows the flow direction, and the blue and red arrows show the Coriolis and curvature forces, respectively. On the dusk side the Coriolis

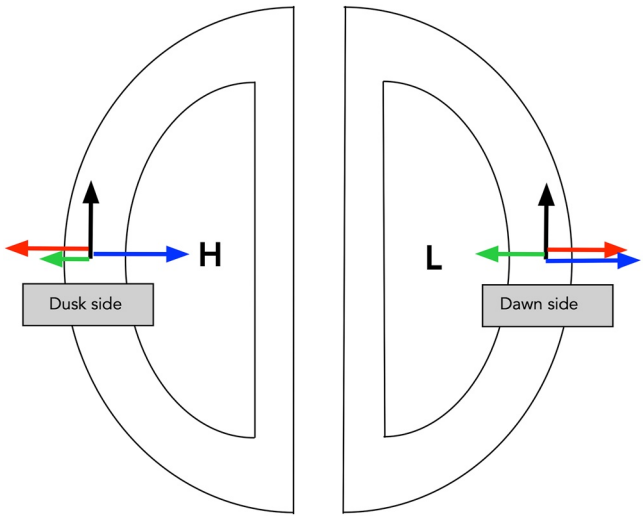

Figure 3. Schematic diagram showing the flow directions for the two physical roots of the gradient wind equation corresponding to normal cyclonic and anticyclonic flow presented in the context of the two-cell convection pattern. The blue arrows show the direction of the Coriolis force, the red arrows the curvature force direction, and the green arrows the pressure gradient force.

and curvature terms are in opposite directions, but are in the same direction on the dawn side, making the balance inherently more difficult to achieve on the dawn side.

The heavy dark line in Figure 4 shows the behavior of the magnitude of all four physical solutions. In the figure, the normal solution is the portion below the $V_{gw} = 2V_{geo}$ extremum. The anomalous solution is the portion of the curve above the extremum and is only relevant for anticyclonic flow, as we will discuss further below. In the graph V_{geo} represents the pressure gradient in the form of an equivalent geostrophic wind. The curve therefore shows that the gradient wind increases as the pressure gradient increases up to the point where the gradient wind is twice the geostrophic value. Beyond that the gradient wind continues to increase as the geostrophic value, that is, the pressure gradient decreases, with the gradient wind eventually reaching a maximum value when the gradient wind is equal to the inertial wind, that is, when the curvature and Coriolis terms balance each other. The pressure gradient is zero at that point.

A clearer picture of the dynamics responsible for the limits discussed above can be seen in the diagram of the forces for the anomalous gradient wind solutions in Figure 5. As shown, the flow direction for both anomalous solutions is anticyclonic. There is no cyclonic flow solution for the case that $V_{gw} > 2V_{geo}$. In terms of the actual high-latitude flow, accelerating the neutrals beyond the $2V_{geo}$ speed would require a reversal of the neutral flow direction on the dawn side, that is, a change in direction to motion opposite the direction of the forcing due to the Pedersen Lorentz force. In the auroral oval, the Lorentz forcing associated with the two-cell convection pattern creates an anticyclonic circulation on the dusk side and a cyclonic circulation on the dawn side. Because the cyclonic solution is limited to the normal gradient wind, the maximum wind on that side is $V_{gw} = 2V_{geo}$. By contrast, the solutions on the evening side extend to the full V_{iner} value, which is twice as large. The implication is that there is an inherent asymmetry in the magnitude of the winds that can be supported on the dusk and dawn side with a difference of approximately a factor of two.

The scenario for the generation of winds on the dusk side is the following. Initially when the forcing is imposed, the Coriolis force will be dominant. Since the strong westward forcing occurs within a channel with a narrow north-south extent, the winds within the channel are displaced to the right by the Coriolis force, that is, poleward in this case. Winds outside the channel are small, and the result is the build-up of back pressure near the poleward boundary. This tends to keep the flow in the acceleration channel where the magnetospherically-imposed Lorentz force is large. As the wind speed increases, the centrifugal force becomes more important. The maximum pressure gradient occurs when $V_{gw} = 2V_{geo}$. Beyond that point, the pressure gradient decreases, and the wind continues to increase, finally reaching its maximum value of V_{iner} if the forcing persists long enough. If the forcing continues to act, the winds could be expected to increase further, but if there is no balance of forces beyond the critical value, any additional acceleration will result in inertial instability, leading to the generation of waves and a reduction of the wind speed to the inertial wind value. We can calculate an approximate value for the limiting wind speed as follows. The effective radius for the centrifugal force for a circulation centered at the pole is $R_E \tan\theta$, where R_E is the radius of the Earth and θ is the co-latitude. The radius can be smaller in a smaller-radius circulation, but the value estimated here should be reasonable for a circulation generated by the two-cell convection pattern. For $\theta = 25°$, the inertial wind speed is ~350 ms^{-1}, which is close to the value measured in the two cases presented above as examples. It is questionable

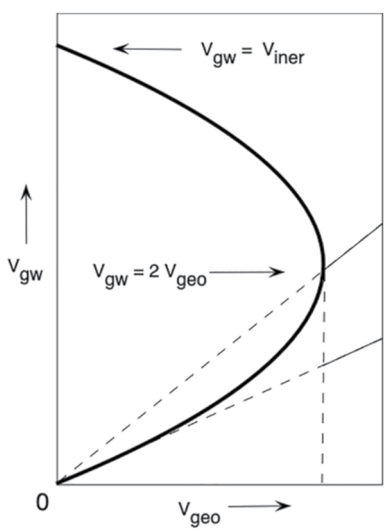

Figure 4. Plot of the the gradient wind solution on the vertical axis versus the geostrophic wind on the horizontal axis. Note that the geostrophic wind represents the equivalent pressure gradient.

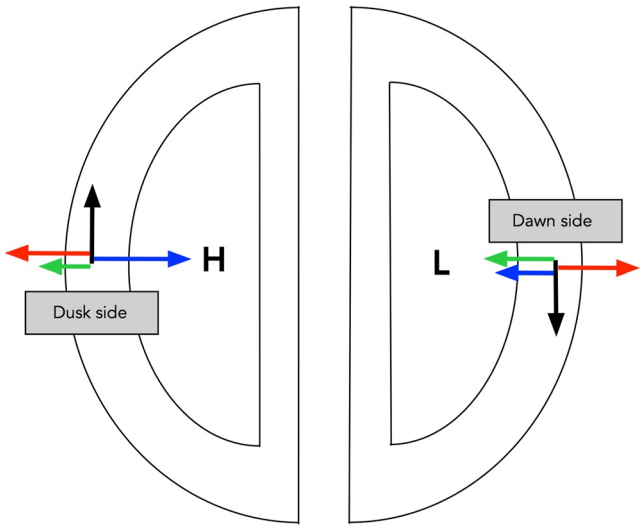

Figure 5. Schematic diagram showing the flow directions for the two physical roots of the gradient wind equation corresponding to the anomalous flow cases in the same format as Figure 3.

whether wind speeds much larger than this can be supported by the high-latitude lower-thermospheric flow in the auroral oval.

4. MIST Launches

The Mesospheric Inversion Stratified Turbulence (MIST) rockets included two vapor tracer rockets launched on 26 January 2015, approximately 30 min apart. The first launch was at 2210 MLT. The primary goal of the experiment was to study mesospheric turbulence, but conditions were active throughout the night. The launches therefore provided information about the dynamics in the lower *E*-region, as well as information about turbulence lower down. In addition the two launches provided information about the temporal evolution of the flow. Figure 6 shows the up- and down-leg wind profiles for the first launch and the down-leg profile for the second launch. The first profile shows features similar to those of the two previous examples with large peak winds between 125 and 130 km altitude. Of particular interest is the meridional gradient in the meridional wind shown by the winds in the top and center panel. Specifically, the meridional wind decreased with latitude at the time of the first launch, suggesting that there was convergence along the direction toward north, increasing the southward directed pressure gradient force. At the time of the first launch, the up-leg zonal winds peaked with maximum speeds close to 300 ms^{-1}, that is, in the range corresponding to the anomalous gradient wind solution. An increasing pressure gradient moves the solution to the right along the curve in the top half of Figure 4, leading to a decrease in the gradient wind speed. A half hour later, the wind speeds have decreased significantly in the altitude range where the meridional advection was significant. The change in the winds is not likely to be entirely due to a change in the pressure gradient, but it is reasonable to expect that it would be a contributing factor.

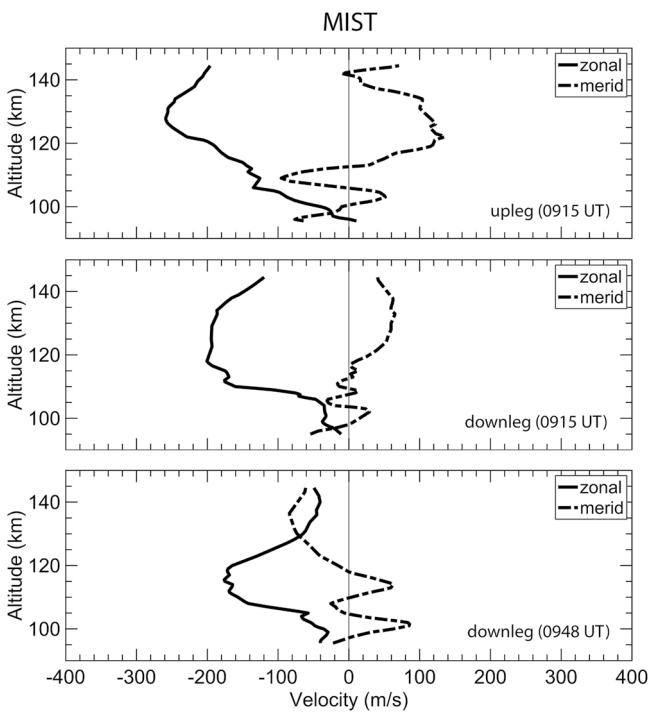

Figure 6. The three panels show the up-leg (top) and down-leg (middle) wind profiles for the mesospheric inversion stratified turbulence launch at 0915 UT on 26 January 2015 plus the upleg profile at 0948 UT, approximately half an hour later.

5. Discussion and Summary

The gradient wind balance applies to any curved flow and is common in the lower atmosphere in connection with the meridional excursions associated with Rossby waves and the associated jet streams. The wind speeds are generally small enough, however, so that the balanced solutions are limited to the normal cyclonic and anticyclonic gradient wind solutions. The anomalous solutions, if they exist, are much less common, but a series of papers for well over half a century have argued that they can occur in the troposphere in special circumstances (Alaka, 1961; Brill, 2014; Cohen et al., 2017; Fultz, 1991; Godson, 1949; Gustafson, 1953; Knox & Ohmann, 2006; Krishnamurti et al., 2005; N. Li, 2015; T. Li et al., 2017; Mogil & Holle, 1972; Willoughby, 2011). The requirement for making the anomalous solutions viable is a large sustained forcing that can push the winds past the $2V_{geo}$ limit. Those conditions are difficult to obtain in the lower atmosphere, with the possible exception of certain mesoscale phenomena, including tropical cyclone forcing. The situation is quite different, however, in the auroral oval where the forcing is imposed externally from the magnetosphere. As long as the Lorentz forcing is sustained, the acceleration can continue and the winds can be accelerated to the anomalous gradient wind balance regime and even to the limit imposed by the basic balance of forces, that is, the inertial wind limit. The numerical model results from the Kwak and Richmond (2007) study represent integrations carried out to steady state and show wind speeds on the dusk side that are close in magnitude to the inertial wind limit. The observational examples presented here represent samples during the transient adjustment phase since they occur after a few hours or less of forcing. Nonetheless,

the examples from 1978 show maximum winds close to or at the inertial wind limit with relatively small meridional flow, indicating that the winds were close to the adjusted state.

Gradient wind balance has not been explored quantitatively in the context of the mesosphere and lower thermosphere flow with the exception of the study by Lieberman (1999) of mid- and low-latitude winds measured by satellite, which found a near gradient wind balance, but with winds limited to values that would be characteristic of the normal rather than the anomalous solution. The anomalous solution was not considered, as would be expected, since winds outside the auroral oval are generally not large enough to satisfy the anomalous solution balance condition.

The discussion and analysis in the previous sections have focused on the Pedersen component of the Lorentz force as a driver for the neutrals, that is, an ion push, but the meridional flow perpendicular to the plasma drifts also experiences a corresponding drag due to the Pedersen component of Lorentz force. Larsen and Mikkelsen (1983) showed that the effect of the meridional drag is to reduce the time required to reach the adjusted state by damping the oscillatory motions that are a natural part of the adjustment process. The same increases in the plasma density that increase the acceleration of the flow therefore also make the adjustment required to keep the flow in the acceleration region more efficient.

A related point is that the Hall component of the Lorentz force is significant in the lowest part of the *E*-region. As shown by Larsen and Walterscheid (1995), the Hall drag term at high latitudes where the magnetic field lines are near vertical creates a deflection perpendicular to the neutral flow direction but opposite to that of the Coriolis force. The net effect can be treated as a reduction in the Coriolis parameter with an effective f given by the Hall drag coefficient subtracted from the actual Coriolis parameter. As the Hall drag coefficient increases with height up to a peak value near 120 km (see, e.g., Larsen & Walterscheid, 1995, Figure 1), the inertial wind value, and therefore also the maximum wind value that can be supported, will be less below that altitude than above.

A final point is that the meridional pressure gradient is an important part of the gradient wind balance but is difficult to measure. Nonetheless, we can infer the likely behavior of that parameter from the gradient wind relation. In particular, the actual adjustment process during the transient acceleration phase for the flow will be subject to oscillations as the mass field is redistributed by meridional advection. Joule heating can also affect the horizontal mass and pressure distribution. The pressure gradient therefore cannot be expected to align exactly to the parabolic curve that is the solution of the gradient wind equation (Figure 4). Nonetheless, the upper limit given by the inertial wind value depends only on the Coriolis parameter f and the radius of curvature R. The lower limit is zero. In between there has to be an increase in the pressure gradient leading to the maximum for the normal solution and a decrease in the gradient associated with further acceleration of the winds. The implications of the results presented here are therefore that on both the dusk and dawn side of the auroral oval, a horizontal pressure gradient increase created by the flow adjustment process must accompany the acceleration of the neutral flow. The acceleration on the dawn side is limited to twice the geostrophic value. The flow on the dusk side can increase further, however, to an upper limit given by the inertial wind value, which is $\sim$350 ms^{-1}. A further implication is that any process that changes the cross-flow pressure gradient will also lead to changes in the maximum wind speed. On the dawn side the relationship is straightforward since only the normal solution applies. In that case a decrease in the gradient corresponds to a decrease in the gradient wind speed. On the dusk side in the anomalous gradient wind case an increase in the pressure gradient will actually lead to a decrease in the wind speed, which is somewhat counterintuitive.

The real lower thermosphere flow at high latitudes has a complex mixture of forces, including tidal forcing, Joule heating, and the Lorentz forcing that has been the focus here. The gradient wind balance cannot explain all aspects of the observed winds, but it does appear to account for some of the main features, including a limit on the observed wind maxima in the *E*-region and the asymmetry between dusk and dawn flows.

Data Availability Statement

Data files can be accessed at https://doi.org/10.5281/zenodo.5796100

Acknowledgments
The work at Clemson was supported in part by NSF award AGS-2012994 and by NASA grant NNX14AH09G. R. Mesquita acknowledges partial support from internal JHUAPL funding.

References

Alaka, M. A. (1961). The occurrence of anomalous winds and their significance. *Monthly Weather Review*, *89*, 482–494. https://doi.org/10.1175/1520-0493(1961)089<0482:tooawa>2.0.co;2

Brill, K. F. (2014). Revisiting an old concept: The gradient wind. *Monthly Weather Review*, *142*, 1460–1471. https://doi.org/10.1175/mwr-d-13-00088.1

Cohen, Y., Harnik, N., Heifetz, E., Nolan, D. S., Tao, D., & Zhang, F. (2017). On the violation of gradient wind balance at the top of tropical cyclones. *Geophysical Research Letters*, *44*, 8017–8026. https://doi.org/10.1002/2017GL074552

Crowley, G., Immel, T. J., Hackert, C. L., Craven, J., & Roble, R. G. (2006). Effects of imf by on thermospheric composition at high and middle latitudes. *Journal of Geophysical Research*, *111*, A10311. https://doi.org/10.1029/2005JA011371

Fuller-Rowell, T. J., & Rees, D. (1981). A three-dimensional, time-dependent simulation of the global dynamical response of the thermosphere to a geomagnetic substorm. *Journal of Atmospheric and Solar-Terrestrial Physics*, *43*, 701–721. https://doi.org/10.1016/0021-9169(81)90142-2

Fultz, D. (1991). Quantitative nondimensional properties of the gradient wind. *Journal of the Atmospheric Sciences*, *48*, 869–875. https://doi.org/10.1175/1520-0469(1991)048<0869:qnpotg>2.0.co;2

Galperin, B., & P. L. Read (Eds.), (2019). *Zonal jets: Phenomenology, genesis, and physics*. Cambridge University Press. https://doi.org/10.1017/9781107358225

Godson, W. L. (1949). Some remarks concerning the gradient wind equation. *Bulletin of the American Meterological Society*, *30*, 342–346. https://doi.org/10.1175/1520-0477-30.10.342

Gundlach, J. P., Larsen, M. F., & Mikkelsen, I. S. (1988). A simple model describing the nonlinear dynamics of the dusk/dawn asymmetry in the high-latitude thermospheric flow. *Geophysical Research Letters*, *15*, 307–310. https://doi.org/10.1029/gl015i004p00307

Gustafson, A. F. (1953). On anomalous winds in the free atmosphere. *Bulletin of the American Meterological Society*, *34*, 196–201. https://doi.org/10.1175/1520-0477-34.5.196

Heppner, J. P., & Miller, M. L. (1982). Thermospheric winds at high latitudes from chemical release observations. *Journal of Geophysical Research*, *87*, 1633–1647. https://doi.org/10.1029/ja087ia03p01633

Holton, J. R. (1992). *An introduction to dynamic meteorology*. Academic Press.

Knox, J. A., & Ohmann, P. R. (2006). Iterative solutions of the gradient wind equation. *Computers & Geosciences*, *32*, 656–662. https://doi.org/10.1016/j.cageo.2005.09.009

Krishnamurti, T. N., Cunningham, P., & Rajendran, K. (2005). Anomalous gradient winds in the subtropical jet stream and interpretation of forecast failures. *Meteorology and Atmospheric Physics*, *88*, 237–250. https://doi.org/10.1007/s00703-004-0075-x

Kwak, Y.-S., & Richmond, A. D. (2007). An analysis of the momentum forcing in the high-latitude lower thermosphere. *Journal of Geophysical Research*, *112*(A01306). https://doi.org/10.1029/2006JA011910

Larsen, M. F., & Mikkelsen, I. S. (1983). The dynamic response of the high-latitude thermosphere and geostrophic adjustment. *Journal of Geophysical Research*, *88*(3158–3168). https://doi.org/10.1029/ja088ia04p03158

Larsen, M. F., & Walterscheid, R. L. (1995). Modified geostrophy in the thermosphere. *Journal of Geophysical Research*, *100*, 17321–17329. https://doi.org/10.1029/95ja00137

Li, N. (2015). A discussion on the existence of the anomalous high and the anomalous low. *Annales Geophysicae*, *33*, 1253–1261. https://doi.org/10.5194/angeo-33-1253-2015

Li, T., Wang, B., Wu, B., Zhou, T., Chang, C.-P., & Zhang, R. (2017). Theories on the formation of an anomalous anticyclone in western north pacific during el nino: A review. *Journal of Meteorological Research*, *31*, 987–1006. https://doi.org/10.1007/s13351-017-7147-6

Lieberman, R. S. (1999). The gradient wind in the mesosphere and lower thermosphere. *Earth Planets and Space*, *51*, 751–761. https://doi.org/10.1186/bf03353234

Mesquita, R. (2021). *An observational investigation of mid-latitude thermospheric temperatures and high-latitude E*-region neutral wind structures (Unpublished doctoral dissertation). Clemson University.

Mikkelsen, I. S., Jørgensen, T. S., Kelley, M. C., Larsen, M. F., & Pereira, E. (1981). Neutral winds and electric fields in the dusk auroral oval, 2. theory and model. *Journal of Geophysical Research*, *86*, 1525–1536. https://doi.org/10.1029/ja086ia03p01525

Mikkelsen, I. S., Jørgensen, T. S., Kelley, M. C., Larsen, M. F., Pereira, E., & Vickrey, J. (1981). Neutral winds and electric fields in the dusk auroral oval, 1. measurements. *Journal of Geophysical Research*, *86*, 1513–1524. https://doi.org/10.1029/ja086ia03p01513

Mogil, H. M., & Holle, R. L. (1972). Anomalous gradient winds: Existence and implications. *Monthly Weather Review*, *100*, 709–716. https://doi.org/10.1175/1520-0493(1972)100<0709:agweai>2.3.co;2

Walterscheid, R. L., & Boucher, D. J. (1984). A simple model of the transient response of the thermosphere to impulsive forcing. *Journal of the Atmospheric Sciences*, *41*, 1062–1072. https://doi.org/10.1175/1520-0469(1984)041<1062:asmott>2.0.co;2

Willoughby, H. E. (2011). The golden radius in balanced atmospheric flows. *Monthly Weather Review*, *139*, 1164–1168. https://doi.org/10.1175/2010MWR3579.1